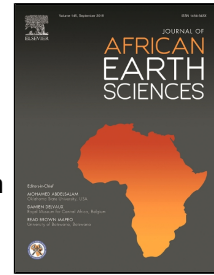


Accepted Manuscript

Drivers, patterns and velocity of saltwater intrusion in a stressed aquifer of the East African coast: joint analysis of groundwater and geophysical data in Southern Kenya.



Oiro Samson, Comte Jean-Christophe

PII: S1464-343X(18)30269-3
DOI: 10.1016/j.jafrearsci.2018.08.016
Reference: AES 3305
To appear in: *Journal of African Earth Sciences*
Received Date: 14 February 2018
Accepted Date: 24 August 2018

Please cite this article as: Oiro Samson, Comte Jean-Christophe, Drivers, patterns and velocity of saltwater intrusion in a stressed aquifer of the East African coast: joint analysis of groundwater and geophysical data in Southern Kenya., *Journal of African Earth Sciences* (2018), doi: 10.1016/j.jafrearsci.2018.08.016

This is a PDF file of an unedited manuscript that has been accepted for publication. As a service to our customers we are providing this early version of the manuscript. The manuscript will undergo copyediting, typesetting, and review of the resulting proof before it is published in its final form. Please note that during the production process errors may be discovered which could affect the content, and all legal disclaimers that apply to the journal pertain.

1 *Drivers, patterns and velocity of saltwater intrusion in a stressed aquifer*
2 *of the East African coast: joint analysis of groundwater and geophysical*
3 *data in Southern Kenya.*

4 *Oiro Samson^{1,2,*}, Comte Jean-Christophe¹*

5 *1 University of Aberdeen, School of Geosciences, Scotland, United Kingdom.*

6 *2 Water Resources Authority, Government of Kenya*

7 *Corresponding author: Samson.Oiro@abdn.ac.uk*

8 ***Key words***

9 Coastal aquifer system, Seawater Intrusion, Electrical Resistivity Tomography, Recharge, Groundwater
10 time series

11 ***Abstract***

12 Fresh groundwater resources in coastal East Africa are crucial for the region's socio-economic
13 development but are under threat of salinization caused by changes in recharge patterns and increasing
14 abstraction. With the aim of establishing the drivers behind saltwater intrusion and its current spatial
15 extent, we studied the Kenyan South Coast aquifer, a representative, strategic aquifer under increased
16 pressure. Investigations included electrical resistivity tomography (ERT) surveys and in-situ
17 groundwater measurements (water table and basic quality) together with the analysis of available long-
18 term climatic and borehole monitoring data. Over the last 40 years, groundwater electrical conductivity
19 values at the well field increased by about three times and groundwater levels declined by 1 to 3 m over
20 the last decade. When put in perspective with the long-term climate (rainfall, temperature) and
21 abstraction records, these trends in groundwater appear to be primarily driven by increased borehole
22 abstraction (+400 m³/day per year in average), whereas observed increasing temperature (+0.02 °C per
23 year) and decreasing rainfall (-0.8 mm per year) could potentially act as a secondary control through
24 reduced recharge. However the low statistical significance obtained for both rainfall and temperature
25 trends over the observation period suggests that no clear conclusion can be made with regards to long-
26 term climate impact on groundwater. Groundwater quality mapping showed that proximity to the ocean,

27 presence of abstraction well-fields and regional geology control groundwater salinity patterns at regional
28 scale. Locally, geophysical data showed that, saltwater intrusion spatial patterns are controlled by local
29 aquifer lithology, groundwater abstraction and freshwater recharge in floodplains. Comparison with
30 previous (1984) resistivity data showed that the saltwater front has advanced toward the well-field by
31 up to 2 km and rose by up to 80 m over the last 30 years, which corresponds to a maximal velocity of
32 about 60 m/y horizontally and 2 m/y vertically. Implementation of groundwater management strategies
33 such as sustainable groundwater exploitation, sourced alternative water supply, and managed aquifer
34 recharge are required to mitigate the effects of seawater intrusion along the East African coastal strip.

35

36 *1. Introduction*

37 About half of the global population resides within coastal areas (IPCC and UNEP, 1997; Jahanshahi
38 and Zare, 2016; Sonkamble et al., 2014), most of them, particularly in the developing world being
39 subject to high demographic increase resulting in higher groundwater demand. In these areas,
40 groundwater is a vital freshwater resource for human needs (Ketabchi et al., 2016) and the broader
41 environment through acting as exchange zones separating marine and terrestrial hydro-biogeochemical
42 cycles (Colombani et al., 2015; Post and Werner, 2017). They are highly sensitive to changes triggered
43 by both natural and anthropogenic forcing such as climate, land use, pollution and over-pumping
44 (Comte et al., 2014; Hsieh et al., 2015; Iyalomhe et al., 2015; Klassen and Allen, 2017; Lathashri and
45 Mahesha, 2015). The use of coastal groundwater for drinking, agriculture or industry is however globally
46 compromised by the salinization problem (Ahmed et al., 2017; Argamasilla et al., 2017; Himi et al.,
47 2017). Progressing saltwater intrusion into freshwater aquifers due to over-abstraction have prompted
48 global alert and concern (Ahmed, 2017; Priyanka and Mahesha, 2015; Sonkamble et al., 2014).
49 Salinization due to over-abstraction leads, in the most severe cases, to water supply wells being
50 abandoned (Argamasilla et al., 2017; Himi et al., 2017; Ketabchi et al., 2016; Klassen and Allen, 2017;
51 Post and Werner, 2017). Aquifer recharge reduction caused by climate change is another important
52 factor of salinisation (Green et al., 2011; Singh et al., 2014).

53 In Africa, over 50% of population live in coastal zones (Altchenko and Villholth, 2013; Arthurton, 1998;
54 Steyl and Dennis, 2010) with freshwater demand as a basic human need being at centre stage
55 (Arthurton, 1998; Steyl and Dennis, 2010; Taylor et al., 2012). Human developments strongly affect the

56 coastal strip hydrosystems with 38% of the African coast categorized by UNEP in 1998 as under severe
57 threat from over-development (Steyl and Dennis, 2010). In Sub-Saharan coastal areas particularly,
58 higher resilience of groundwater than surface water systems to the impacts of climate change and
59 pollution is promoting rapid, unprecedented development of groundwater resources, which in turn
60 increases their dependability by population (Steyl and Dennis, 2010). Groundwater data scarcity and
61 lack of high level interstates cooperation has been pointed out as major obstacle in managing Africa's
62 coastal aquifers of which many are transboundary (Steyl and Dennis, 2010; Wangati and Said, 1997).
63 Yet improved management of groundwater resource requires acquisition of suitable groundwater
64 inventory information including assessment of groundwater limiting factors, and how to disseminate the
65 information for the benefit of coastal communities (Arthurton, 1998).

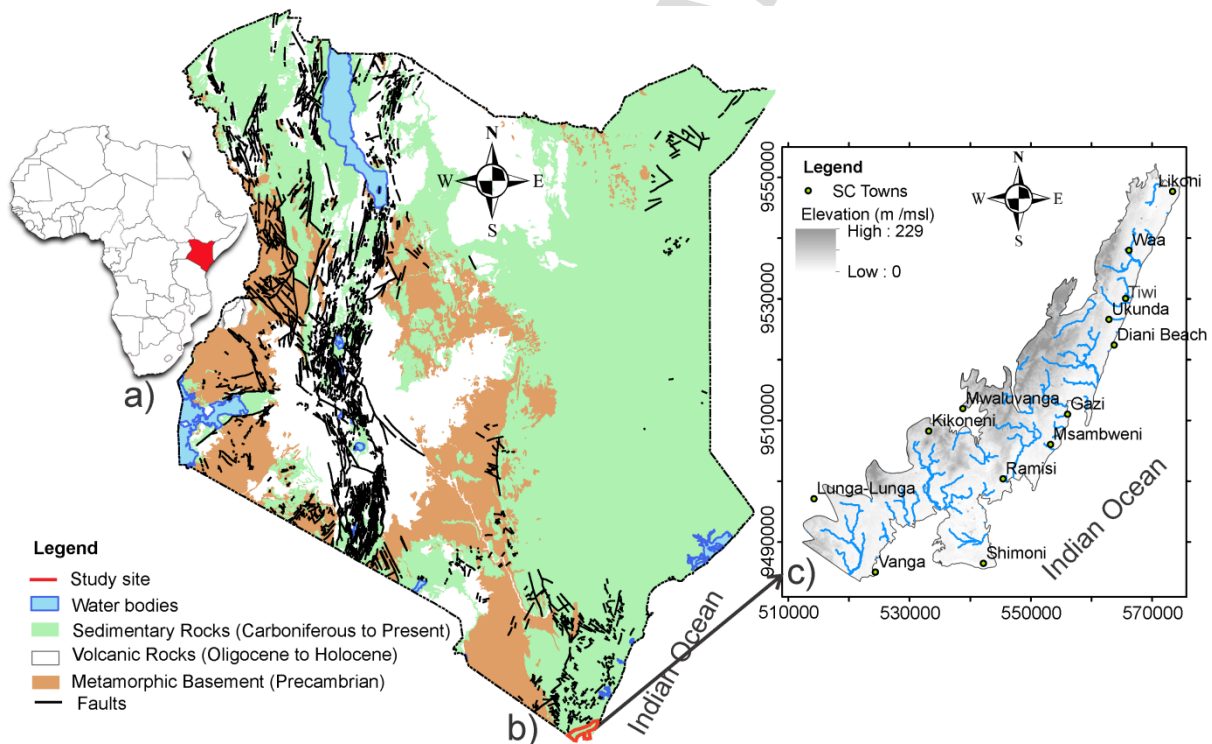
66 In East Africa more specifically, coastal aquifers are the main source of freshwater supply for all the
67 economic sectors and domestic use and groundwater exploitation has increased with time (Comte et
68 al., 2016). In Kenya, supply of quality freshwater was flagged long ago as a major challenge facing the
69 coastal communities with problem intensity dependent on seasons (Arthurton, 1998). Up to 1972, most
70 water boreholes within south coast of Kenya, which supported over 0.5 Million people including the
71 major city of Mombasa, were drilled in the coastal fringe areas underlain by Pleistocene coral reef.
72 Saline contamination is greatly pronounced in areas of coral limestone (Tole, 1997) due to high
73 permeability and low hydraulic gradients resulting from large primary porosity and secondary
74 karstification. After 1972, less saline sandy facies aquifers of back-reef/lagoon origin (Magarini and
75 Kilindini sands), located further inland, were explored and drilled (Buckley, 1981). The first borehole in
76 1973 was installed near the Tiwi village and was then followed by other eight exploratory wells with two
77 being able to be used for production yielding good quality and quantity water (Buckley, 1981). The so-
78 called Tiwi Aquifer is among the highest yielding sedimentary-rock aquifers of Kenya (Wangati and
79 Said, 1997). The Kenyan south coast aquifer system (Tiwi) is also amongst the most threatened
80 aquifers in East Africa by seawater intrusion fashioned by groundwater over-exploitation (Tole, 1997;
81 Wangati and Said, 1997).

82 The research aimed at assessing the current extent, past evolution and drivers of coastal aquifer
83 salinization in the East African coast using climatic records, current and historical groundwater
84 monitoring data including basic in-situ measured water quality parameters and geophysical (electrical
85 resistivity tomography – ERT) investigations in the Kenyan South Coast aquifer. The specific objectives

86 of the groundwater mapping and geophysical investigations were: (1) understanding the regional impact
 87 of the observed changing climate and groundwater abstraction on freshwater availability and saltwater
 88 intrusion; and (2) delineating sub-regional and local spatial patterns and evolution of seawater intrusion
 89 into the main exploited aquifer systems.

90 2. Study area

91 The study area is located in Kwale County, on the Kenyan South Coast, East Africa. It lies within one
 92 of the five major catchment areas of Kenya, the Athi River catchment. The altitude ranges from 0 m
 93 near the ocean to 229 m inland, within latitude $4^{\circ} 1.5'$ to $4^{\circ} 40.6'$ S, and longitude $39^{\circ} 5.4'$ to $39^{\circ} 43.2'$
 94 E. Slightly less than a million people live in the Kwale County, however, groundwater from the area
 95 supports over 1M people in two counties of Kwale and Mombasa. The population density of the area
 96 varies from 70 people/km² in rural villages to over 4000 persons/km² in towns along the coastline
 97 (Mombasa included).



98
 99 **Figure 1:** General physical maps showing (a) the location of Kenya within the African continent (b) the
 100 simplified geology of Kenya and (c) the South Coast study area indicating topography (grey scale), main
 101 rivers (blue lines) and main towns (small circle).

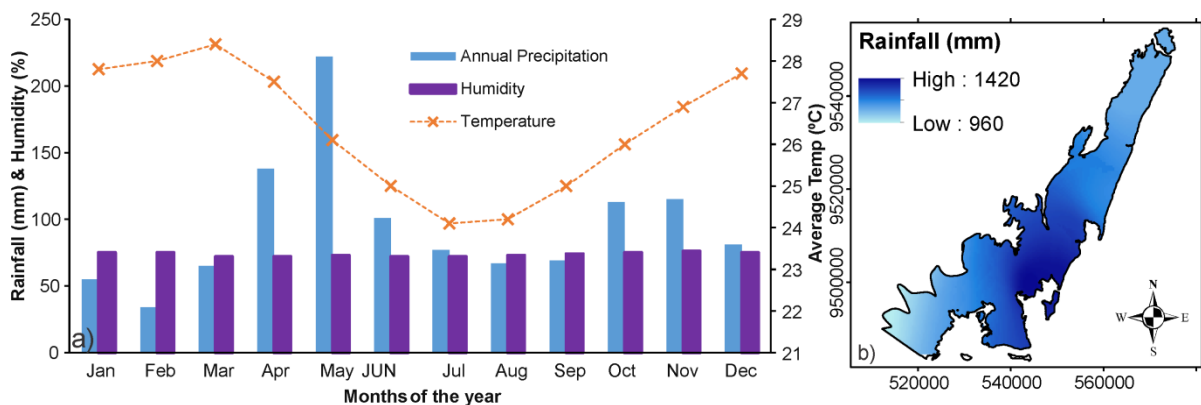
102

103

104

2.1. Climate

105 The South Coast (SC) coastal aquifer system experiences an equatorial coastal climate characterised
 106 by warm and humid conditions. The annual average temperature is 27°C with a mean maximum and
 107 minimum temperatures of 30°C and 23°C, respectively. The warmest months run from October to April
 108 and are associated with ample rains (Adams, 1986; Carruthers, 1985; Mwakamba et al., 2014; Tole,
 109 1997). Monthly average humidity within the year oscillates between 70% and 77%. The area
 110 experiences bi-modal rainfall distribution with the main wet season (long rains) extending from April to
 111 June and the less pronounced short rains from October to December (see Fig. 2a). The annual average
 112 precipitation derived from Moi International Airport Mombasa meteorological station, within the study
 113 area amounts to 1100mm with some disparity between years. Adams (1986) attributed inland gradual
 114 decline in rainfall to the controls by south-easterly winds (Fig. 2b).



115

116 **Figure 2:** (a) average monthly precipitation (mm), humidity (%), and temperatures (degrees Celsius)
 117 variations over the last 40 years; (b) spatial variations of average annual rainfall over the SC aquifer.

118

2.2. Hydrogeology

119 Successive geological mapping of the area was conducted by Gregory (1921), Miller (1952), Caswell
 120 (1953), Thompson (1956) and Buckley (1981). Sequential sedimentary rock formations occupy the
 121 region with decreasing Pliocene to Pleistocene age towards the Indian Ocean coastline (Kuria, 2013).
 122 The general striking trend of geological formations is parallel to the coastline on a SSW – NNE direction
 123 and dipping to the east (Adams, 1986; Carruthers, 1985; Kuria, 2013) (Fig. 3). Msambweni and Tiwi
 124 well fields are the two most exploited pumping sites within the area (Fig. 3). They form part of a larger

125 aquifer complex, the so-called South Coast aquifer system mainly composed, in a West-East sequence,
126 of Magarini sands (Pliocene), Kilindini sands (Pleistocene) and the coral reef platform (Pleistocene
127 reef), which are recharged by rainfall due to unconfined sedimentary formations over the area (Buckley,
128 1981). The Magarini sands form a coastal terrace overlying mostly impermeable Jurassic shales, which
129 outcrop to the West (Adams, 1986; Carruthers, 1985; Wangati and Said, 1997). Boreholes logs also
130 reported presence of cretaceous limestones beneath the coastal fringe coral reef, which are preserved
131 thanks to normal faulting affecting the pre-Pliocene sedimentary formations. According to Carruthers
132 (1985), the depth of the top of the Jurassic shale beneath the coastal plain is greater than 100 m.
133 Fluctuating sea level during the Pleistocene contributed to landward partial erosion of the Pliocene
134 Magarini Sands terrace and subsequent deposition of a new sedimentary terrace complex. The complex
135 includes a thick fossil coral reef limestone fringing the Indian Ocean to the East, which reaches more
136 than 100 m thickness near Mombasa (Adams, 1986), transitioning to back-reef fluviatile, deltaic,
137 lagoonal and aeolian sediments (the so-called Kilindini Sands) to the West (Buckley, 1981; Carruthers,
138 1985). According to borehole logs (Carruthers, 1985) the Pleistocene aquifer complex directly lies on
139 the Jurassic and Cretaceous aquitard formations.

140 Msambweni and Tiwi well fields are located within the Pliocene Magarini and Pleistocene Kilindini
141 sands, respectively. The Kilindini Sands (Pleistocene back-reef sand deposits) display the highest
142 groundwater potential in the South coast (Adams, 1986; Buckley, 1981; Carruthers, 1985; Mumma et
143 al., 2011; Tole, 1997). At the Tiwi well field, they are among the highest groundwater yielding, abstracted
144 sedimentary formations of Kenya. At the scale of the South Coast aquifer, the Kilindini sedimentary
145 facies displays lateral variations (Adams, 1986; Buckley, 1981; Carruthers, 1985; Tahal and Bhundia,
146 2012). The physical aquifer properties are summarised in Table 1.

147 The average recharge of the Tiwi aquifer has been previously estimated to equal 23% of annual rainfall
148 by several authors (Adams, 1986; Carruthers, 1985; Wangati and Said, 1997). Temporarily flowing river
149 beds and floodplains are reported to be responsible for direct recharge to the sands as they dry out
150 before reaching the Ocean (Carruthers, 1985).

151 Observed water levels in the aquifer are fluctuating above the mean sea level, from about 1 m near the
152 Ocean to 10 m inland (Mumma et al., 2011). The water table slopes gently towards the coast where
153 groundwater discharges (Buckley, 1981). The existence of a saline water interface in freshwater

154 discharge areas implies that a decline in groundwater flow through the aquifer caused by exploitation
 155 and/or reduced recharge promotes inland advancement of the interface and/or saline water up-coning
 156 below abstraction points (common in areas of thin freshwater lenses with shallow saline water) which
 157 may lead to wells being abandoned (Buckley, 1981).

158 The overall groundwater flow rate within the Tiwi aquifer from its northern to southern ends (about 13
 159 km in length) (Fig. 3) was estimated to be 100,000 m³/day (4200 m³/hr) by Wangati and Said (1997)
 160 using Darcy's law through hydraulic gradient analysis.

161

162 Table 1: Summarised Tiwi aquifer properties as derived from past studies.

Authors	Hydraulic Conductivity		Transmissivity		Storativity S	Recharge (% of annual rainfall)	
	Kilindini sands	Reef limestone	Kilindini sands	Reef limestone		Kilindini sands	Reef limestone
(Adams, 1986)	-	-	85 - 700	-	4 x 10 ⁻² - 8 x 10 ⁻²	23	13
(Wangati and Said, 1997)	-	-	85 - >300	2000- 5000	-	-	-
(Buckley, 1981)	15 - 36	-	850 - 2000	-	9.3 x 10 ⁻³	-	-
(Mumma et al., 2011)	13 - 36	-	120 - 600	-	9.3 x 10 ⁻³ - 9.9 x 10 ⁻²	-	-

163

164

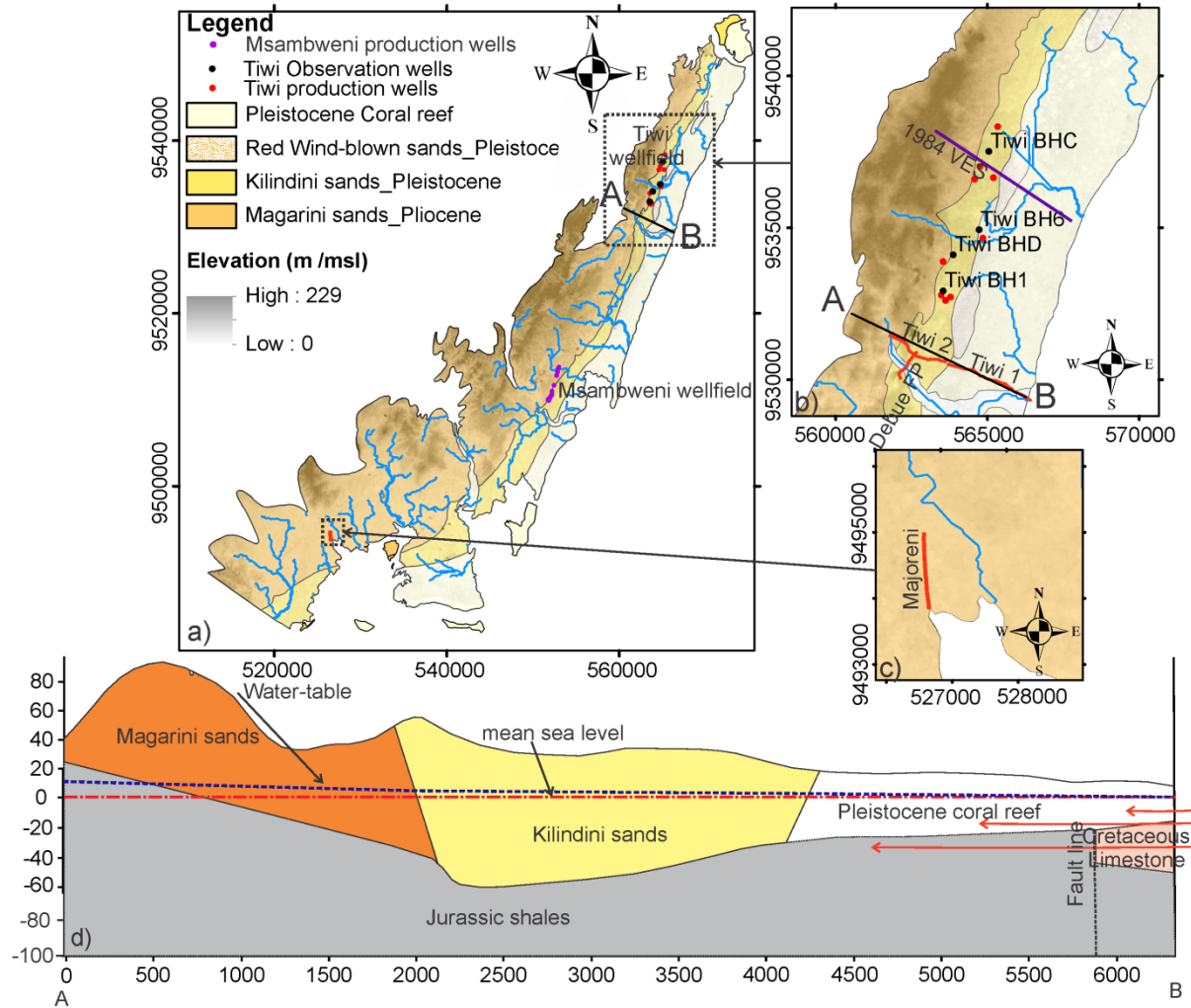
165

166

167

168

169



170

171 **Figure 3:** (a) Geological map of the study area with ERT profile lines in red and the two main well-fields
 172 labelled, (b) Enlarged section of the 2017 ERT profiles including Tiwi 1, Tiwi 2, Debue flood plain, as
 173 well as the 1984 VES profile in purple, (c) enlarged section of the Majoreni ERT transect, and (d)
 174 hydrogeological cross-section cutting across Tiwi wellfield (in meters) with red arrows showing seawater
 175 intrusion direction (from Adams 1986).

176

3. Methodology

177

3.1 Climate data analysis

178 The historical climate data available for eleven weather stations across the coastal region were
 179 purchased from the Kenya Meteorological Department (Head Office, Nairobi). The nearest station from
 180 the study site (Moi International Airport, Mombasa; average annual rainfall of 1200 mm) had

181 precipitation data available from 1970 to 2016 (46 years), and temperature data from 1972 to 2016 (44
182 years). Data were compiled, re-organized, and analysed using linear regression to highlight climate
183 trends over the last decades and possible future projections. The total annual rainfall was first calculated
184 from the monthly records to highlight the long-term inter-annual variations. Temperature records
185 contained both the maximum and minimum monthly averages of which annual averaged maximum and
186 minimum temperature were generated and plotted against the observation year. Linear regressions
187 were subsequently applied to the three time-series (annual rainfall, average min temperature and
188 average max temperature) to highlight and assess possible long-term trends over the observed period.
189 Statistical analysis using linear regression was performed on the climate data using SPSS Statistics
190 version 20 software. The data were grouped in 10 years period to test if there are decadal variations
191 using nonparametric test. The implications of the results on possible trends of evapotranspiration,
192 groundwater recharge and storage were then discussed. Finally, the monthly records (rainfall and
193 temperature) were compared to the groundwater time-series for the more recent period (2011-2017) for
194 which groundwater records were available.

195 *3.2 Spatiotemporal groundwater data analysis*

196 Monitored groundwater levels and quality are primary source of information on groundwater dynamics
197 and hydrologic stresses exerted on aquifers (Taylor and Alley, 2001). Existing monitoring groundwater
198 data, including temporally monitoring wells and spatial monitoring networks, were compiled in order to
199 perform temporal analyses and new piezometric mapping, respectively.

200 *3.2.1 Piezometric mapping*

201 116 water table measurements were collected and analysed during July 2016, using an electric
202 groundwater level dip meter. Measurement of geographical coordinates were captured using a hand-
203 held GPS (GPSMAP 76CSx with +/- 5 m accuracy, which implies an error on X,Y well locations of less
204 than 0.1% over the 13 km x 85 km study area). Most of the sampled points were open wells (56 in
205 number) and monitoring piezometers (4 in Tiwi well-field). Groundwater levels were measured with
206 respect to ground surface level using cm-accurate dip meter and subsequently converted to absolute
207 elevation (in reference to mean sea level) using the digital elevation model of 30 m by 30 m resolution,
208 which has a vertical accuracy of 1 m. Other records from boreholes completion reports obtained from
209 WRA Mombasa Office were compiled and the static water levels (147 borehole records) were added to

210 the measured levels during sampling. As temporal variations of the water table were found to be much
211 lower than spatial variation at the regional scale, we deemed acceptable to combine water level records
212 from historical reports with the 2016 dataset. The interpolation of water table measurements, performed
213 using kriging interpolation tools in ArcGIS, produced a regional piezometric surface map highlighting
214 the mean regional groundwater flow directions.

215 *3.2.2 Groundwater quality mapping*

216 3 spring water and 106 groundwater points (wells and boreholes) were sampled for groundwater quality
217 concurrently to water table measurements in July 2016. This included basic water quality parameter
218 (pH, TDS, EC, Salinity, Turbidity, and temperature) as measured with a WAGTECH portable multi-
219 parameter kit provided by the Kenyan Water Resources Authority (WRA). Most samples were collected
220 from the highly productive geological units of sands (Magarini and Kilindini and karst limestone (Plio- to
221 Pleistocene units) with a few from older low-yielding sandstones (Maji ya Chumvi Permo-Triassic
222 formation) outcropping in the southwest of the area. Samples were collected in 500ml plastic bottles
223 and analysed on site. The plastic sampling bottles were cleaned with distilled water prior to use.
224 Georeferencing of sampled points used the same procedure as for water levels (see previous section).
225 For the scope of this work we only present EC (microS/cm) data.

226 *3.2.3 Analysis of groundwater and abstraction time series*

227 The long-term groundwater monitoring in Kenya, including water level and electrical conductivity, is
228 primarily undertaken by the WRA, at devolved sub-regional level. In the Tiwi aquifer, four wells are
229 actively monitored monthly since 2007 for water levels and since 2012 for electrical conductivity (EC).
230 Monitoring data are archived by the WRA Coastal Office (Mombasa). Recorded values of dynamic water
231 level and electrical conductivity were plotted over time to which linear regressions and a moving average
232 regression respectively were applied to highlight possible temporal trends resulting from the impact of
233 continued groundwater exploitation within the wellfield.

234 Abstraction records in south coast is highly fragmented as most of the abstraction points (open wells
235 and hand-pumped wells) are not metered. On another hand, existing records from metered boreholes
236 in Tiwi well-field are incomplete; only monthly records for the period October, 2007 to December, 2012
237 are available at the WRA. This limitation prompted the use of abstraction rates for the Tiwi well-field

238 only based on the information from technical reports of the area (Adams, 1986; Buckley, 1981;
239 Carruthers, 1985; Sincat-Atkins, 1996; Tahal and Bhundia, 2012). It is reported that the number of
240 production wells increased from two (2) in 1973 to thirteen (13) in 2013. The combined abstraction data
241 were extracted for year 1972, 1975, 1979, 1994, 1996, 2012 and 2017. During 2016 fieldwork, few new
242 non-metered community boreholes, drilled after 2014 were encountered within the Tiwi well-field and
243 groundwater abstraction from them as per 2017 was estimated and plotted together with those extracted
244 from reports for metered boreholes. The resulting graph was then used in comparison with other
245 analyses (climatic, groundwater level and quality observation) to understand driving factors behind
246 changing groundwater quantity and quality of south coast area.

247 *3.6 Geophysical investigations*

248 The geophysical technique of electrical resistivity tomography (ERT) is a popular technique for
249 delineation of aquifer boundaries and architecture as well as saltwater-freshwater interface and mixing
250 in coastal aquifer systems, which includes examples of successful application in coastal East Africa
251 (e.g. Comte et al, 2016).

252 ERT was implemented in February 2017 through deployment of four profiles (4 ERT lines) (Fig. 3 a -
253 c). The roll-along procedure was applied to extend the length of the initial 360m lines. Tiwi1 profile (Fig.
254 3 a & b) ran for 3.4 Km from the main road down to the ocean next to Mwachema River mouth. The
255 profile was expected to provide insights on the contact between Pleistocene Kilindini sands formation
256 and Pleistocene coral reef, the possible influence of Mwachema River into the aquifer, the thickness of
257 the freshwater lens, and the extent of seawater intrusion from the coast. Tiwi 2 profile (Fig. 3 a & b) was
258 2.5 Km long, West to, and in line with, Tiwi1 and cut across both the Pliocene Magarini sands and
259 Pleistocene Kilindini sands; the latter being the main aquifer formation. It intended to help delineating
260 the geological boundary between the two formations, the true aquifer thickness, and the patterns of
261 seawater intrusion. Debue flood plain profile (Fig. 3 a & b) was 1.2 Km and carried out within a river
262 floodplain incised by a tributary of Mwachema River that experiences perennial flooding. This profile
263 was intended to provide information on the relation between the river and the aquifer. Majoreni profile
264 (Fig. 3 a & c) was 1.2 Km long and was carried out in the south of the studied region where the Magarini
265 sands outcrop and are in direct contact with the sea.

266 Each profile comprised an array of 72, 5-m spaced, stainless steel electrodes connected to a Syscal
267 Pro Switch 72 10-channels transmitter/receiver system (Iris instruments). This configuration permitted
268 a total depth of investigation of about 75 m. Two quadripole arrays (injection and measurement dipoles)
269 were sequentially used; the Dipole-Dipole (DD) and multi-gradient (mGD) arrays. To improve galvanic
270 contacts between electrodes and the dry soils and therefore reduce the noise, the electrodes were
271 watered with brackish water. Electrodes positions were recorded using a hand-held GPS and the
272 elevation of each electrode points were later extracted from the 30 m x 30 m DEM. Obtained DD and
273 mGD apparent resistivities were separately processed (noise filtered) and subsequently jointly inverted
274 using the program RES2DINV v3.59 from Geotomo Software (Loke and Barker, 1996) in order to
275 provide a 2D vertical distribution model of true subsurface resistivity. The profile topography was
276 included in the inversion. The quality of fit between calculated apparent resistivities (from the inverse
277 model) to measured apparent resistivities was evaluated using root mean square (RMS) error.

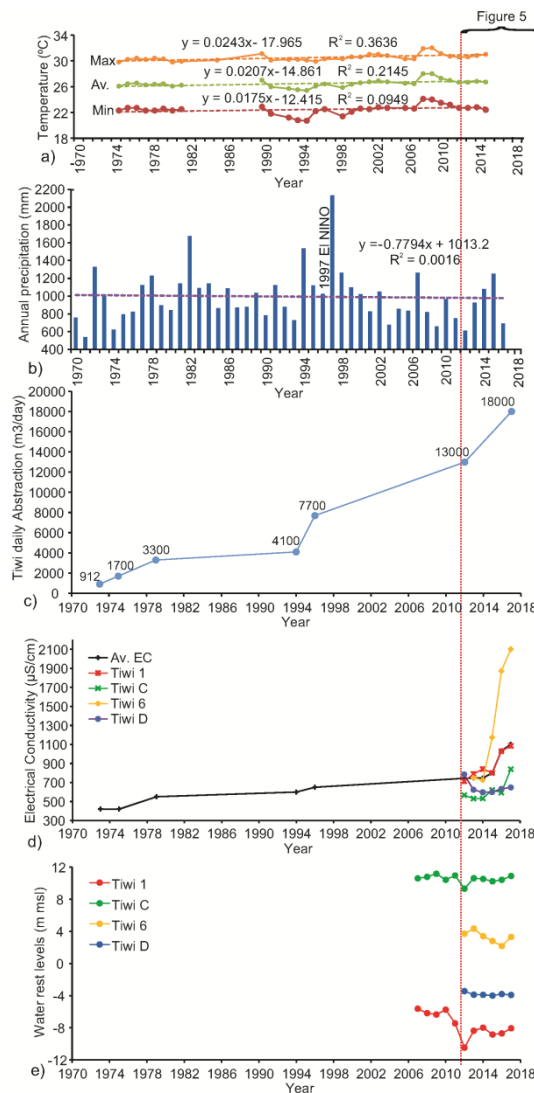
278 Previous geophysical data (vertical electrical soundings VES and airborne electromagnetics) from
279 Carruthers (1985) were also included in the analysis to highlight possible changes in geophysical
280 properties between then and now, related to changes in groundwater conditions (water table and
281 saltwater intrusion). The nearest VES transects (regularly-spaced 1D electrical soundings) from the
282 1985 Carruthers report, named transects 1+2 in the report, were digitised and re-interpolated in 2D
283 (cross-section) to compare with the 2017 ERT cross-section (Tiwi 1+2). To produce a 2D interpolation
284 from the 1D VES profiles, each VES was tabulated with respect to altitude, model resistivity, and
285 distance from the coastline. VES distance from coastline was obtained from their longitude and latitude
286 coordinates recovered from the ArcGIS georeferencing of the Carruthers (1985) map. The altitude of
287 both the ground surface and the VES resistivities were calculated from the average depth of the VES
288 model layers and their ground elevation as extracted from DEM.

289 4. Results

290 4.1. Long-term climatic trends

291 The analysis of annual precipitation over the last 45 years revealed significant interannual variability
292 with periods of heavy annual rainfall occurring at an average frequency of 10 years, which correspond
293 to the major El Nino (high rainfall) events. The El Nino effect is particularly clear in 1982 and more
294 spectacularly in 1997. Over the whole period, rainfall displays an almost insignificant decreasing trend,

295 at an average rate of 0.8 mm per annum (Fig. 4b). Annual temperatures are less variable over time and
 296 display a slight increasing trend of 0.02 °C/year since 1972 (Fig. 4a).



297

298 **Figure 4:** (a) Annual mean average, minimum, and maximum temperature from 1972 to 2016, and
 299 linear trend showing slightly increasing temperatures at the rate of 0.02°C /year, (b) 1970 to 2016 annual
 300 precipitation record with linear decreasing trend of 0.8 mm/year, (c) 1973-2017 estimated daily
 301 abstraction rate of Tiwi aquifer, (d) 1973-2017 EC records averaged over Tiwi aquifer from boreholes
 302 reports plotted with the 2011-2017 annually averaged EC for individual observation wells, and (e) 2007-
 303 2017 annually averaged groundwater levels from individual observation wells. Monthly records for the
 304 period 2011-2017 are presented in more details in Figure 5.

305 Linear regression analysis using SPSS demonstrates statistically insignificant and slightly significant
 306 change in annual rainfall and mean annual temperature, respectively. This is indicated by the low

307 regression R-squared values, below 0.3, as presented in table 2 and in Figure 4 a & b. Excel linear
 308 regression analyses yielded strictly identical statistical results. Such low statistical significances imply
 309 that the calculated linear trends of decreasing rainfall (- 0.85 mm/year) and increasing temperature
 310 (0.02 °C/year) do not allow for confidently drawing conclusions on climate trends over the 50 years
 311 observation period and its possible impact on groundwater recharge and seawater intrusion. The
 312 nonparametric test yielded no variations between compared decadal climatic data thereby highlighting
 313 the insignificance of the climatic change effect on groundwater over observation period at 0.05
 314 significance level.

315 Table 2: SPSS linear regression output for the analysed climatic data

SPSS output	Annual Rainfall	Mean annual Temperature
Slope	-0.854	0.021
R- Squared	0.002	0.215
R	0.040	0.463
95% Confidence Interval	-7.333 - 5.625	0.006 - 0.036

316

317 4.2. Groundwater historical evolution

318 Abstraction of groundwater within the south coast is on the rise since its inception. However, most
 319 abstraction is not recorded as open wells and hand-pumped wells are not metered yet they constitute
 320 the highest numbers of abstraction points. To get a glimpse of the abstraction in the area, Tiwi wellfield
 321 groundwater development abstraction is considered for simplification. Observation made from Figure 4
 322 c and 5 c reveals an increasing trend. Figure 5 c shows an increase of daily abstraction rate from 12500
 323 m³ in 2011 to 18000 m³ in 2017. The increase can be linked to increased water demand driven by
 324 unprecedented population growth within the area.

325 Recent observations plotted on Figure 5 a & b, demonstrate strong seasonality of temperature and
 326 rainfall with temperature increase before the onset of heavy (long) rains, typical between November
 327 and March. The same is also observed in the multi-decadal records of Figure 4 a & b, before the El
 328 Nino event. This is explained by high temperatures leading to high evaporation over the ocean and
 329 increased vapour in the atmosphere, which eventually results in increased rainfall after condensation.

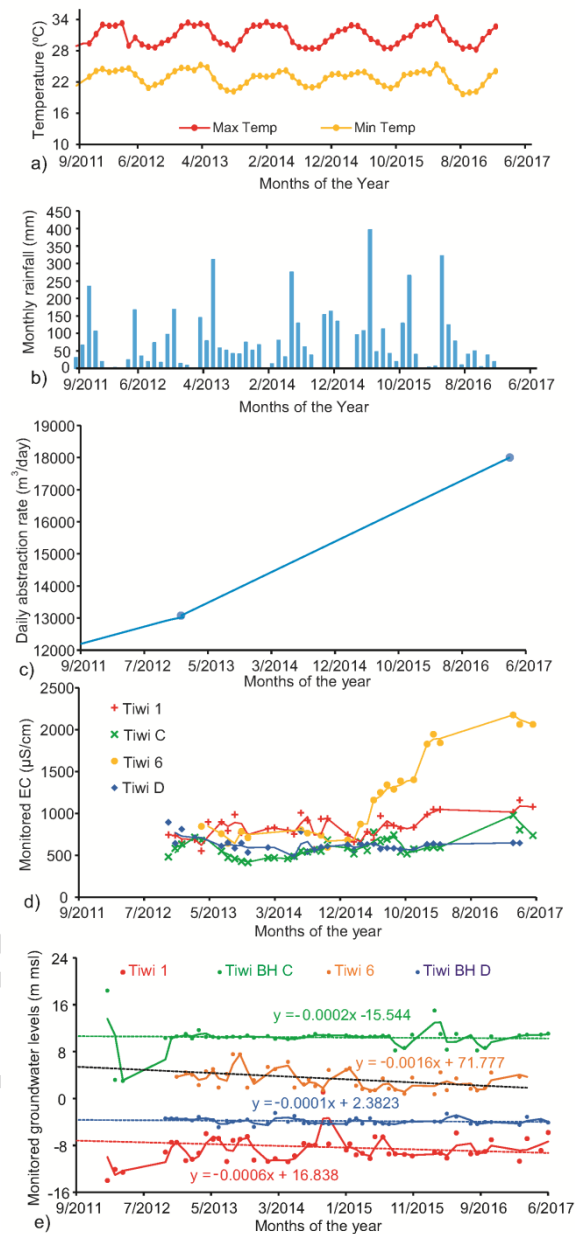
330 Observations made from borehole basic quality monitoring data over the last years showed an
 331 increasing electrical conductivity, an indication of saltwater influence/groundwater quality deterioration

332 (Fig. 4d & Fig. 5d). The records of average EC over the Tiwi production wells between 1972 and 2017
333 show an overall increase from about 400 $\mu\text{S}/\text{cm}$ to 1100 $\mu\text{S}/\text{cm}$, which closely mirrors the abstraction
334 increase (900 to 18,000 m^3/d combined). Individual borehole records from 2011 show the same
335 similarity. Both suggest that groundwater abstraction is the primary contributing factor to increasing EC
336 and saltwater intrusion. In more details, in the 2011-2017 monthly records (Fig. 5d), EC values for Tiwi
337 6 borehole showed a sharp rise starting in 2015, from steady values of about ~ 800 $\mu\text{S}/\text{cm}$ to over 2000
338 $\mu\text{S}/\text{cm}$ in 2017, which seems to continue. This equates to an EC increasing rate of about +500 $\mu\text{S}/\text{cm}$
339 per year and again mirrors the increase in groundwater abstraction. Tiwi 1 and Tiwi C also showed an
340 increasing EC, although lower than Tiwi 6, of about ~ 75 $\mu\text{S}/\text{cm}$ per year starting in 2015 and 2013,
341 respectively. These observations contrast with the ones, prior to 2011, made by Mumma et al. (2011),
342 in which they stated that electrical conductivity had not changed significantly since the genesis of Tiwi
343 aquifer development in 1972 (ranging 493 – 1000 $\mu\text{S}/\text{cm}$) to 2011 (ranging 420 – 750 $\mu\text{S}/\text{cm}$). The
344 overall deteriorating quality trend is also affected by seasonal fluctuations attributed to rainfall events
345 (Fig. 5b) (recharge after rains indicated by drops in EC) and perhaps to a local shift in the groundwater
346 flow directions when pumps are not active during shut down.

347 Similar seasonal fluctuations are observed in water table monitoring data, along with an overall inter-
348 annual declining trend over the last 10 years (Fig. 4e & 5e). Across the 4 monitored boreholes, the
349 average decline in groundwater level ranges between 1 m and 3 m over the last 10 years (Fig.5e). The
350 increase of groundwater abstraction from 1000 m^3/day in 1973 to over 15000 m^3/day currently (Tiwi
351 wellfield alone) in this area (Fig.4c and Fig.5c) is driven by domestic and industrial water demands,
352 which are continuously rising as coastal population increases. In 2017, pumping rates have not changed
353 per well and are: 865 m^3/day for Tiwi 1; 715 m^3/day for Tiwi 6; 822 m^3/day for Tiwi C; and 789 m^3/day
354 for Tiwi D but some non-governmental wells has been developed in the area. The monitoring wells
355 respective distance from the ocean is as follows: Tiwi 1 3366 m; Tiwi 6 2876 m; Tiwi C 3724 m; and
356 Tiwi D 3658 m; as shown in Fig. 3. Because abstraction rates do not show large variations between
357 boreholes, it is suggested that the apparent negative correlation between changes in EC and water
358 levels, where wells experiencing the largest decline in water table also exhibit the highest increase (and
359 absolute values) of electrical conductivity, may be primarily linked to the distance from the ocean
360 together with the influence from the active pumping productive wells. This was particularly clear with
361 Tiwi 6 borehole, that has the lowest pumping rate but nearest distance to the ocean compared with

362 other monitoring wells, which produced the highest EC value increase and water table decline. Daily
 363 abstraction has changed from 1973 to now as indicated earlier in response to water demands, this
 364 abstraction change has favoured seawater intrusion through over exploitation of the coastal aquifer and
 365 is gradually becoming a major problem in Tiwi - Diani area (Mwakamba et al., 2014).

366



367

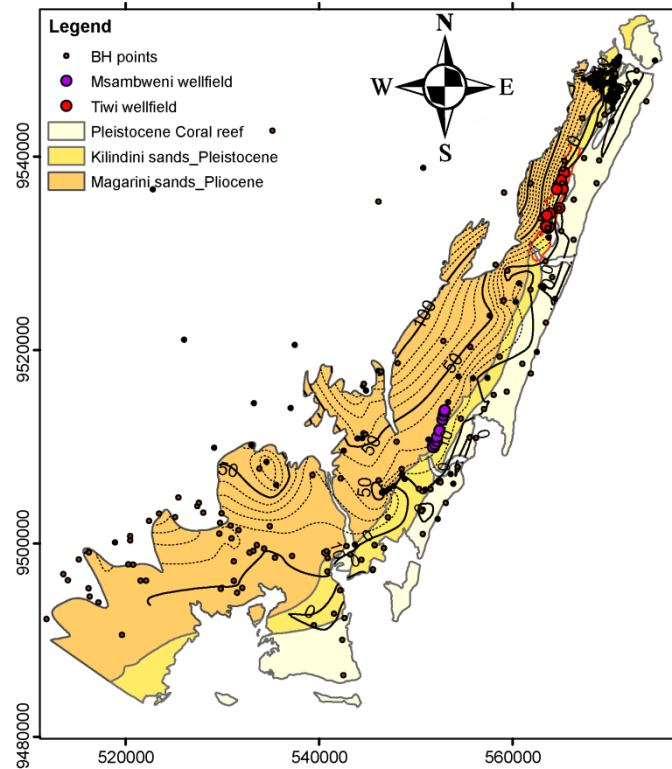
368 **Figure 5:** Detail of records for the period 2011- 2017 (a) monthly average, minimum and maximum
 369 temperature, (b) monthly precipitation recorded at Mombasa airport station, (c) Estimated daily
 370 abstraction rate of the Tiwi well field, (d) Monthly EC recorded at individual observation wells, and (e)
 371 Monthly groundwater levels from individual wells.

372 Overall, the analysis of both long and short temporal records shows close similarity between temporal
373 patterns of increasing EC (and decreasing water level) and increasing groundwater abstraction
374 suggesting that borehole abstraction is the primary driver of saltwater intrusion at both long and short
375 timescales. The lack of clear correlation between seasonal climate variations (rainfall and temperature)
376 and groundwater (levels and EC) suggests that climate variability effect on saltwater encroachment is
377 insignificant as per the available climate data. The slight possibility of decrease in groundwater recharge
378 in long-term scale due to both decrease in rainfall and increase in temperature might be anticipated but
379 not definite.

380 *4.3. Regional groundwater flow directions*

381 The 2016 average potentiometric surface interpolated from water level measurements across the entire
382 SC aquifer ranged from over 100 m on the West to 0 m on the East with reference to mean sea level,
383 with some areas slightly below mean sea level in the coastal fringe (Fig. 6). Regionally, steep
384 groundwater gradients of 0.01 (closely spaced equipotential lines) characterised the Magarini sands in
385 the West part of the aquifer, while the Kilindini sands, coral limestones and the Magarini sands in the
386 far South were characterised by lower gradients of 0.008. Locally, groundwater contour lines also
387 reflected on the impact of wellfields area of influence caused by groundwater withdrawal cone of
388 depression. For instance, lower groundwater heads (and low gradients) were obtained on the eastern
389 side of Tiwi wellfield as compared to Msambweni wellfield. This is explained by higher levels of
390 groundwater abstraction by the Tiwi well field, which produced a significant water table decline that
391 extends towards the coast thereby affecting the natural flow gradient.

392



393

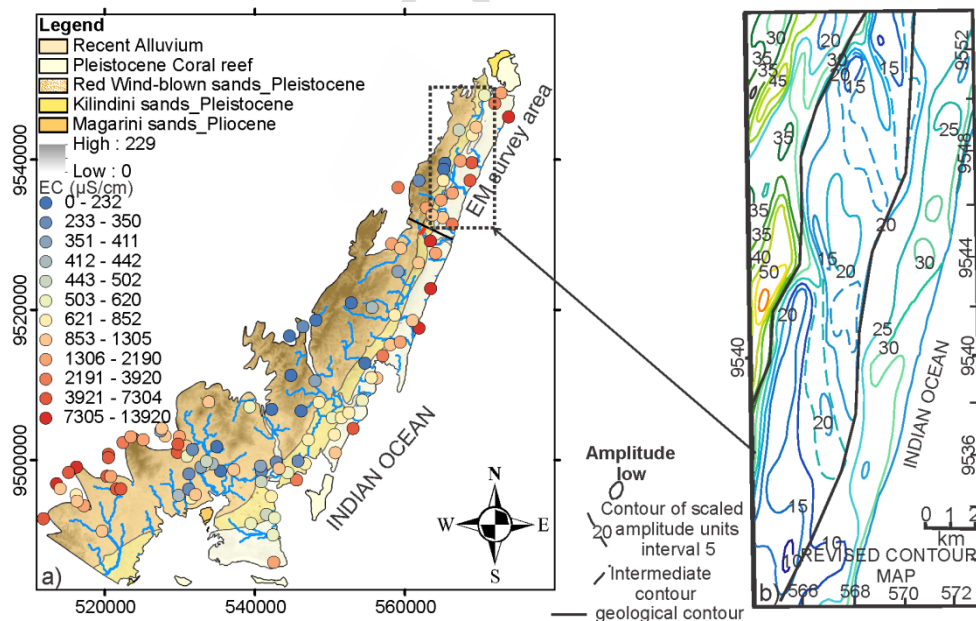
394 **Figure 6:** Potentiometric surface of the study area derived from groundwater levels measured in 2016
 395 and additional data obtained from WRA (± 1 m msl). The two main wellfields in the area are also plotted
 396 with Tiwi on the North and Msambweni on the South, as well as the bedrock geology.

397 4.4. Regional salinity mapping

398 The 2016 map of basic quality parameters illustrates groundwater quality spatial distribution, which
 399 reveals the extent of seawater influence within the aquifer system. Electrical conductivity ranged from
 400 $89 \mu\text{S}/\text{cm}$ – $13920 \mu\text{S}/\text{cm}$ across the study area (Fig. 7 a). Natural controls on the EC values are typically
 401 through seawater intrusion, evapotranspiration and rock mineral dissolution through rock-water
 402 interaction whereas anthropogenic controls are over-abstraction induced seawater intrusion, such as
 403 saline up-coning below well or progressing lateral seawater penetration. The natural control effects
 404 were observed on the Southwest area of which water samples with relatively high EC were collected
 405 on areas under older geological formation of Permo –Triassic Upper maji ya Chumvi beds characterised
 406 by soluble mineral and evaporites ('maji ya chumvi' being a Swahili word for 'salty water') which
 407 increased pore water EC (Oiro et al., 2018). At the coastal fringe however, high EC values (>1000
 408 $\mu\text{S}/\text{cm}$) were attributed to natural saltwater intrusion from the ocean and were mostly restricted to the
 409 coastal reef limestone and part of the back-reef kilindini sands.

410 Previous airborne electromagnetic survey of 1977 (Hetu, 1978), undertaken prior to extensive
 411 groundwater development (Fig. 7b) also yielded high EC values (total aquifer conductivity including
 412 pore water and solid matrix) in areas under the coral limestone as a result of existing saline water at
 413 shallow depth but also within the Jurassic shales due to high clay content. Reduced conductivity was
 414 observed within the back reef sandy facies, which was attributed to freshwater within Kilindini and
 415 Magarini sands (Carruthers, 1985). These data led previous authors (Buckley, 1981; Carruthers, 1985)
 416 to describe the regional extent of the saltwater front as being restricted to the boundary between coral
 417 limestone and Pleistocene Kilindini sands but not recorded as palaeo-saltwater intrusion because of
 418 the natural high contrast in aquifer hydraulic properties; whereby the coral limestone is characterised
 419 by higher hydraulic conductivity resulting in lower hydraulic heads and gradients, and therefore
 420 promoting saltwater intrusion.

421 Comparison of 2016 groundwater data (post groundwater development) with the revised 1977
 422 geophysical data and interpretation (prior groundwater development) therefore suggests that the
 423 seawater intrusion front in the Tiwi wellfield area has progressed inland, from the limestone/Kilindini
 424 boundary to within the Kilindini sands, as a result of over-pumping in order to meet the water demand
 425 of the ever-growing population.



426

427 **Figure 7:** (a) pore water EC in 2016 obtained from groundwater sampling of wells and boreholes, and
 428 (b) total aquifer EC in 1977 obtained from airborne electromagnetic surveys (digitized from, Carruthers,
 429 1985).

430 *4.5. Local patterns of saltwater intrusion*

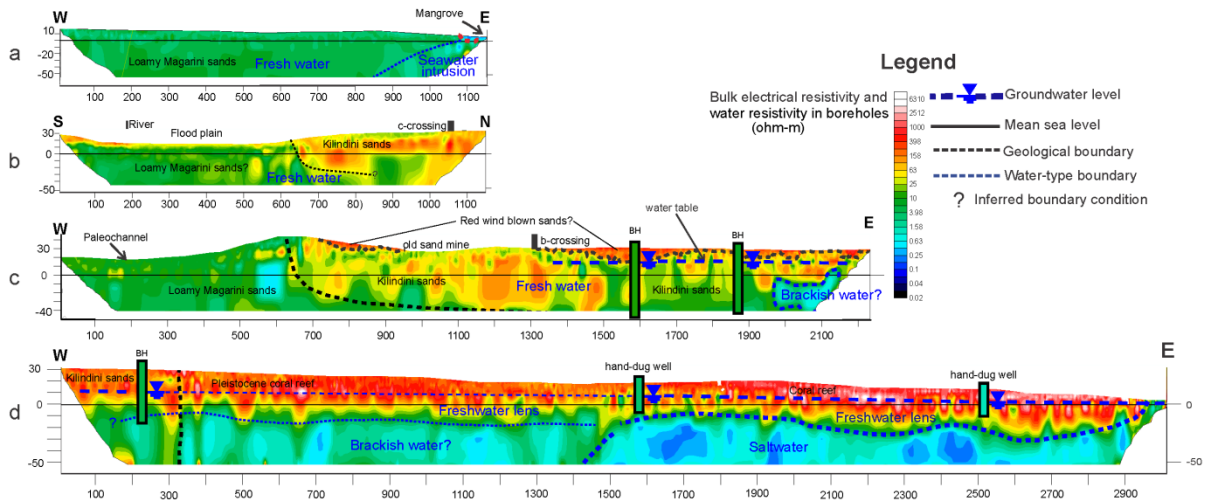
431 The ERT geophysical data captured the patterns of saltwater intrusion with depth along the selected
432 profiles allowing investigating at much higher horizontal and vertical resolution the location of the
433 saltwater front and the influence of lithology and borehole abstraction. Resistivity values characterizing
434 subsurface conditions of the Kenyan south coast were previously described by Carruthers (1985) as
435 follows; (i) 20 – 40 ohm.m for clays, (ii) 2 – 10 ohm.m for Jurassic shales and sands saturated with
436 brackish/saline water, and (iii) 9 – 70 ohm.m representing potable groundwater within clean sand aquifer
437 formation.

438 The new ERT surveys provided true resistivity values ranging from 0.1 ohm.m to over 2500 ohm.m with
439 majority being below 1000 ohm.m (Fig. 8). Large variations in resistivity is shown to reflect both
440 lithological and groundwater salinity variability. The southernmost transect undertaken in Msambweni
441 area (Majoreni profile) was showing relatively low subsurface resistivities (10-20 ohm.m) characteristic
442 of the sand-clay (loamy) facies of the Magarini sands, a relatively poor aquifer system (Figure 8a). The
443 same unit was encountered in the southern half of the floodplain profile (Figure 8b) and the western
444 part of the Tiwi transect (Figure 8c). In Majoreni however the unit was in direct contact with the ocean
445 through an area of low-lying mangroves and displays a decrease in resistivity, to less than 5 ohm.m,
446 towards the mangrove characterised by a relatively steep saltwater intrusion wedge which is consistent
447 with the lower permeability of the Magarini sands. The bank of the flood plain (Figure 8b) and the area
448 where Tiwi well field is installed (Eastern and central part of the profile of Figure 8c) showed higher
449 resistivities ranging about 20 ohm.m to over 200 ohm.m characteristic of cleaner, more water-productive
450 sands, the Kilindini formation. This formation is likely to form a terrace both cutting and overlying the
451 Magarini formation to the West (Figure 8 b & c). The Tiwi transect deployed between the well field and
452 the coastline (Figure 8d) showed high resistivity near the surface (>300 ohm.m) and very low resistivities
453 (<10 ohm.m) below approximate sea level. This transect mostly cross-cut the highly productive coral
454 reef limestone. The high near surface resistivities reflected the unsaturated coral limestones while the
455 lower resistivities underneath reflected the freshwater aquifer and the very lowest at the base of the
456 ERT section reflected the saltwater/brackish water intrusion. There was a general E-W gradient of
457 resistivity resulting from a decrease in salinity from E to W. The approximated transition between fresh
458 and salt/brackish water was not a regular dipping slope toward land but instead, occurred at shallower

459 depths at 3 locations referenced from the coastline: beneath the hotel at ~400m, beneath the village at
460 ~1200m and beneath the most eastern Tiwi market centre at ~2400m. This upward salinity rise was the
461 result of groundwater abstraction causing saltwater 'up-coning'. Up-coning of saline water in south coast
462 was attributed to over exploitation at abstraction point in areas of thin freshwater lenses underlain by
463 saline water near the surface (Buckley, 1981). In the East of the profile at around 300m a lateral change
464 in resistivity likely reflected the transition between the (mostly saline) coral limestone and the (mostly
465 fresh and possibly brackish to the East) Kilindini sands. Consistently Mumma et al. (2011) noted that
466 lateral saline water spreading is most dominant compared to restricted vertical movement. Resistivity
467 values obtained with ERT were broadly consistent with the values provided by Carruthers (1985). In
468 addition, the boundaries of three main geological formations (Magarini, Kilindini and coral limestone)
469 identified with ERT (Tiwi1 and Tiwi2 inverse sections) also produced resistivity boundaries generally
470 consistent with that of the (approximate) mapped geology of the area.

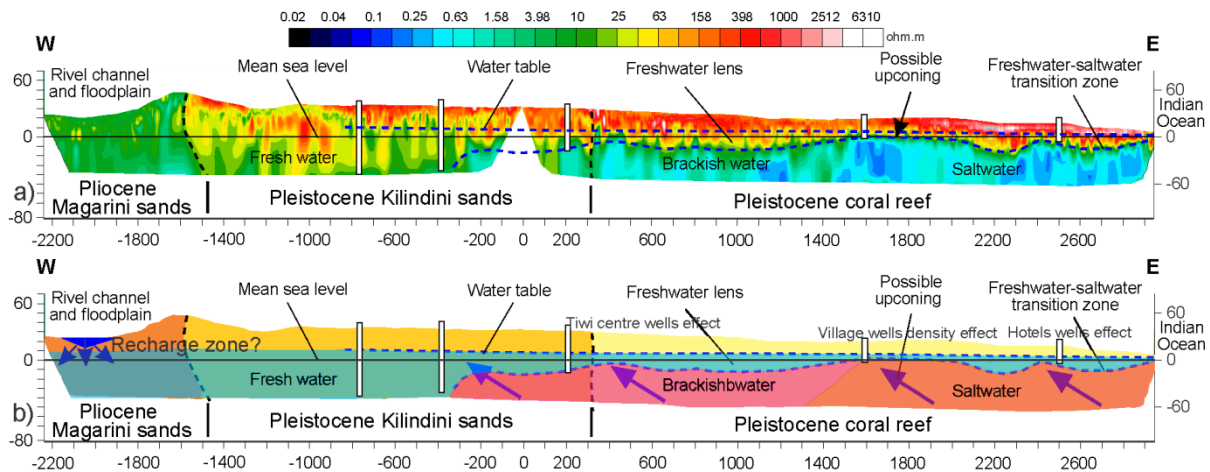
471 In concatenated Tiwi 1 and 2 sections (i.e. after merging the measurements of both sections and joint
472 inversion), the observed low resistivity areas confirmed the 'wave-like' appearance of (saline/brackish)
473 with a total distance of penetration of almost 3 km inland (Fig. 9a). Their correlation with wells/borehole
474 occurrence is typical of saltwater intrusion whereby abstraction reduces the thickness of freshwater lens
475 and promotes saltwater up-coning. Fig. 9b illustrates the interpretative hydrogeological conceptual
476 model derived from the ERT observations.

477 These findings broadly agree with the lower resolution airborne electromagnetic data reported by
478 Carruthers (1985), which yielded high conductivity values in areas under the coral limestone due to
479 presence of saline water at shallow depth along the coast, and within the Magarini loamy sands and
480 Jurassic shales west of the sandy Kilindini facies (Fig. 7b).



481

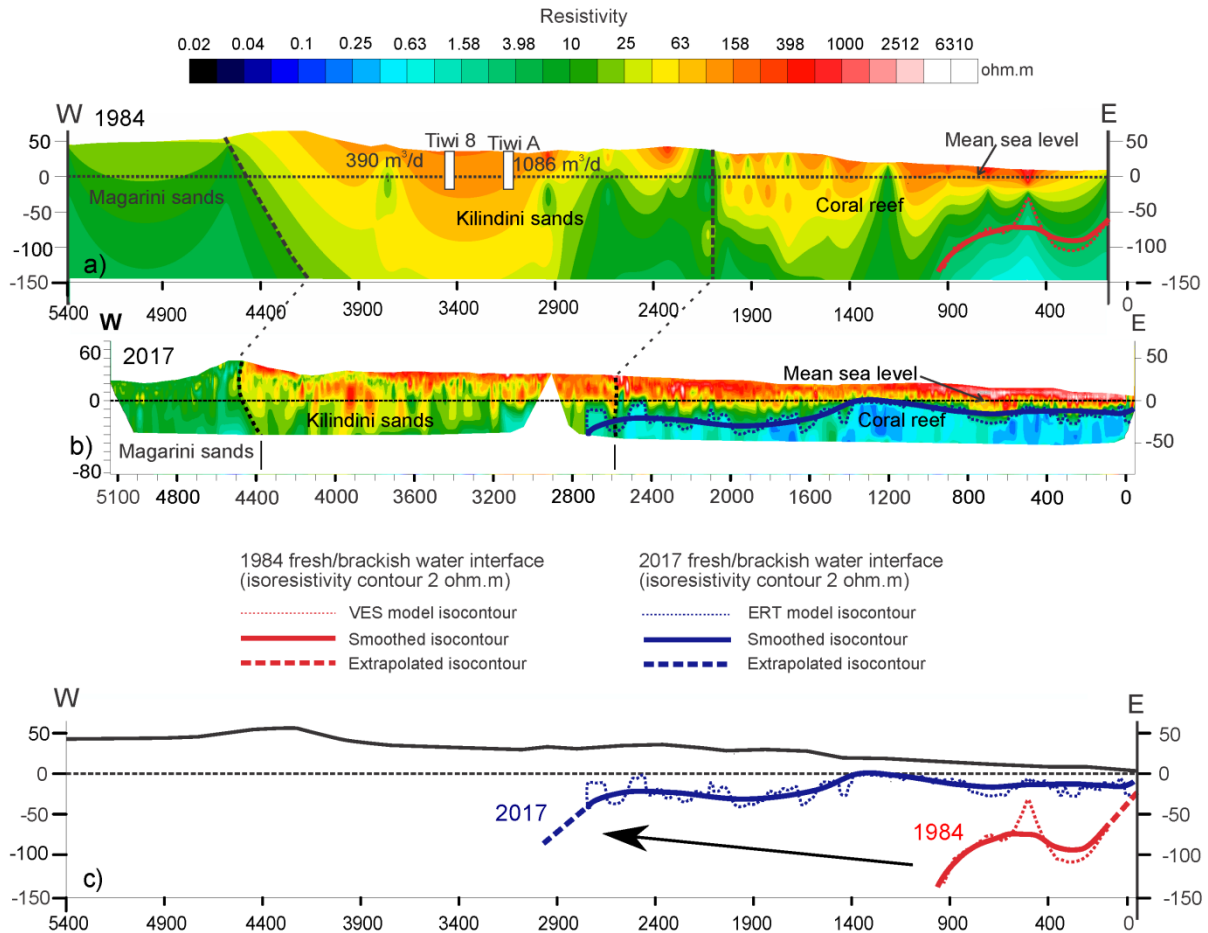
482 **Figure 8:** Inversion results of the ERT profiles with hydrogeological interpretation including geological
 483 units and saltwater distribution (a: Majoreni profile; b: Debye flood plain profile; c: Tiwi 2 profile; and d:
 484 Tiwi 1 profile).



485

486 **Figure 9:** (a) Combined Tiwi1 and Tiwi2 DD profile with hydrogeological interpretation, and (b) derived
 487 conceptual hydrogeological cross-section.

488 A further interpretation of the historical spatio-temporal change, over the last 30 years, of saltwater
 489 intrusion at the Tiwi wellfield was undertaken through comparing the VES (vertical electrical sounding)
 490 results obtained in 1984 on a 5.2 km transect by Carruthers (1985) with the recent (2017) ERT survey
 491 of almost the same length (combined Tiwi1 and Tiwi2 profiles; Fig. 10).



492

493 **Figure 10:** Interpreted geological boundaries and delineation of the brackish water/freshwater interface
 494 in 1984 and 2017 from a) interpolation of the 1984 VES results (Carruthers, 1985) for traverse 1&2 (see
 495 location on Fig. 3) and (b) the 2017 ERT profile (combined Tiwi 1 and 2); and (c) hydrogeological
 496 interpretation of saltwater front displacement over the last 30 years.

497 Using the isoresistivity contour 2 ohm.m as reflecting the seawater front, the comparison of the 1984
 498 and 2017 data suggests that, over the last 30 years, the seawater front has progressed on a horizontal
 499 distance of about 2 km inland (Fig 10c). A vertical shift (rise) of the front, of between 40 m and 80 m,
 500 can also be observed. Using the revised simple Ghyben-Herzberg relationship (Barlow, 2003), which
 501 established that $z = 40h$, where z is the thickness of the freshwater zone below sea level and h as the
 502 freshwater thickness above sea level (i.e. the groundwater head), it was estimated that a vertical rise
 503 of 40 to 80m would correspond to a freshwater head declined of 1 to 2 m. This is very consistent with
 504 the water table and EC observations at the well field over the last decade (Fig. 5), where a drop of 1-3
 505 m was observed concurrently with EC increase. It is however important to note that, although the 2017
 506 ERT transect and the 1984 VES transect were within the same hydrogeological settings, they were not

507 exactly coincident and therefore some uncertainty exist with respect to the exact movement of the
508 saltwater front. It is reasonable to suggest that the geophysical comparison provides a maximum value
509 of displacement of the saltwater front; this because the 2017 profile, unlike the 1984 profile, may be
510 additionally influenced by saltwater entering from the nearby Mwachema river tidal estuary.

511 *5. Discussion*

512 Coastal aquifers are vital for the socio-economic development of towns along the coastal areas (Kenyan
513 coast not exempted) as water needs are met by groundwater exploitation. Understanding factors
514 affecting the sustainability of coastal fresh groundwater resources is crucial. The integrative approach
515 considered under this study in mapping out the extent of seawater intrusion and investigating its driving
516 forces is vital. Widespread problem of seawater intrusion is increasing in coastal aquifers driven by
517 natural causes like sea-level rise and droughts, and by human forces triggering coastal aquifer depletion
518 through over-exploitation (Martínez-Moreno et al., 2017). The observations derived from climatic data
519 suggested a possibility of slightly increasing temperature trend and insignificant decrease in rainfall
520 trend, which in future long-term could impact groundwater recharge negatively through increased
521 evapotranspiration. However, the expected impact of climate change on groundwater resource in the
522 area is statistically minimal if not insignificant. Seawater intrusion monitoring is key to establishing and
523 forecasting coastal aquifer deterioration and enabling means for management purposes (Melloul and
524 Goldenberg, 1997). Quality and water levels observed from monitoring wells further displayed the clear
525 negative impact of groundwater over-exploitation at both long and short term. The water quality was
526 shown to deteriorate over time as EC increases following the same temporal pattern as the increase in
527 abstraction concurrently accompanied by decreasing water levels, which suggests that abstraction acts
528 as a primary driver to saltwater intrusion. In-situ spatial measurements also provided insights on the
529 spatial extent of salinization with higher values reported in wells near the ocean. The quality
530 deterioration concurs with observation made by Tole (1997) who suggested that recent decades of
531 salinization in the Tiwi aquifer was driven by over-exploitation of the coastal aquifer and was gradually
532 becoming a major problem in Tiwi - Diani area (see Fig. 1c for areas mentioned). ERT geophysical
533 surveys revealed the current extent of seawater intrusion into mainland productive aquifer to almost 3
534 Km from the sea downgradient the Tiwi well field. However, areas where poorly productive loamy
535 sediments border the ocean was shown to restrict seawater invasion. Recent geophysical investigation

536 of the status of coastal aquifers in East Africa by Comte et al. (2016) provided similar spatial patterns
537 of salinization in other locations of Kenya and Tanzania. Older works by Gentle (1968) and Carruthers
538 (1985) in the Kenyan South Coast indicated that resistivity values decreased with depth in both the
539 sands and coral units, from hundreds of ohm.m within the unsaturated upper layers to less than 10
540 ohm.m at depths of tens of metres. The methodology applied in this research provided vital information
541 on the extent and changes over time of seawater intrusion and its drivers. It can be replicated in any
542 coastal region characterised by shallow groundwater. ERT method is non-destructive and quick in
543 imaging spatial patterns of seawater intrusion. The results are important for designing monitoring well
544 networks as well as siting wells for productive and sustainable development. The ERT method is also
545 cost effective (Sauret et al., 2015), and can be applied in investigating wider areas (Bosch et al., 2016).
546 Geophysical techniques like ERT however are not solely suitable for investigating point sources of
547 pollution in heterogeneous hydrochemically-controlled coastal environments and require the
548 incorporation of comprehensive chemical scanning techniques such as hydrochemical analyses
549 (Sonkamble et al., 2014), analysis of historical groundwater data, and climatic data. Complementary
550 insights from hydrogeochemical analyses including stable water isotopes and in-situ groundwater
551 quality measurements and their controlling processes can be found in recently published work by Oiro
552 et al. (2018), which supports the current results.

553 Other geophysical techniques have also been successfully applied by other authors to delineate
554 saltwater intrusion in coastal aquifers. Vertical Electrical soundings (VES), which is based on the same
555 principle as ERT but provides data only in 1D (vertical) has been widely applied in detecting and
556 determining saltwater intrusion in layered geological formations (Martínez-Moreno et al., 2017). Time
557 Domain Electromagnetic (TDEM) techniques, also 1D, propagates better beneath highly conductive
558 materials (shallow clay and/or saltwater) and therefore enables in this case to investigate deeper
559 structures and to capture sub-tabular conductive structures (e.g. saltwater) precisely and easily
560 (Martínez-Moreno et al., 2017). The TDEM technique has been applied successfully in mapping
561 seawater intrusion since its first applications in the 1980's (e.g. Goldman et al., 1991). It has also been
562 successful in mapping low-resistivity clay below aquifer systems in Denmark (Danielsen et al., 2003).
563 The frequency domain electromagnetics (FDEM) method is also suitable for detecting high-conductivity
564 bodies in the field but with less vertical resolution than TDEM and ERT and is therefore mostly used for
565 regional mapping (Melloul and Goldenberg, 1997).

566 Groundwater pollution from point sources can be a problem in the study area as ground surface soils
567 of coastal areas (sandy) are well-drained, highly permeable and interconnected coastal aquifer
568 formations thereby promoting contaminant transportation and spreading hence, multiplying coastal
569 aquifer vulnerability and susceptibility to pollution driven by over-pumping (Sonkamble et al., 2014).
570 Poor or non-existence of both liquid and solid treatment plants, and uncontrolled/unmanaged open
571 waste dumping sites is common in developing countries, which favours deterioration of shallow coastal
572 aquifers quality through polluted leachates (Sonkamble et al., 2014), scenarios likely to be largely
573 experienced in Kenyan coast.

574 Based on the findings of this work, the following steps are recommended for future implementation and
575 management of Kenyan south coast aquifer system: 1) spatial distribution of monitoring wells over the
576 region to continue with monitoring both quality and water levels by WRA, 2) carrying out detailed
577 hydrogeochemical analyses of sampled groundwater over the area to provide insights on the extra
578 impact of anthropogenic activities, proper siting, designing and development of future wells to minimise
579 seawater intrusion effect on freshwater, 3) establishing full knowledge of the processes controlling
580 groundwater quality evolution and groundwater flow hydrodynamics of the area, and 4) integrating all
581 the controls and processes affecting the coastal groundwater quantity and quality into groundwater
582 modelling for realizing a sustainable groundwater exploitation and management plan. If the outlined
583 measures are not implemented, fresh water quantity and quality within the south coast aquifer will
584 deteriorate to a point of becoming non-potable, which will have severe socioeconomic implications.

585

586 *6. Conclusion*

587 Population is growing along the coastal areas of Kenya, which is also accompanied by increasing water
588 demand. The water need in the area as well as along the whole, ca. 4000km long East African coast
589 from Somalia to Mozambique is mostly met by exploitation of the coastal groundwater resources. This
590 has pushed both the government and communities to sink more wells ranging from open wells to hand-
591 pumped wells and electric power-driven boreholes. Climatic data recorded over the last few decades in
592 the Kenya South Coast Aquifer, a strategic aquifer for the socio-economic development of coastal
593 Kenya, demonstrated a slightly decreasing precipitation at a slight rate of -0.8 mm per year together
594 with an increasing temperature at the rate of 0.02 °C per year. Statistical analysis of the record however

595 revealed that these trends have low significance and there are no conclusions that can be confidently
596 made on climate trends with the available data. Borehole monitoring observation records have clearly
597 revealed increasing salinity/electrical conductivity and declining water levels by 1 to 3 m, a trend
598 primarily attributed to increasing abstraction of groundwater, with long-term decrease in recharge being
599 a probable secondary factor. This suggests that increased groundwater abstraction is the primary driver
600 controlling deteriorating groundwater quality through saltwater intrusion. Water table was shown to
601 follow, in average, the topographic gradient of the area with local alteration (lower groundwater heads
602 and gradients) in areas under the influence of pumping. High values of electrical conductivity between
603 2000 – 14000 $\mu\text{S}/\text{cm}$ were obtained from measurements made along the coastline and southwest
604 region covered by Permo-Triassic formation of Upper Maji ya Chumvi sandstone. Potable water EC
605 values below 2000 $\mu\text{S}/\text{cm}$ were obtained from the productive sands (Kilindini and Magarini formations).
606 ERT results provided a clear picture of the extent and geological controls on seawater intrusion.
607 Resistivity variations highlighted the subsurface structure by providing information on lithology, depths
608 to water table, freshwater-seawater interface and how far the intrusion has affected the aquifer. A
609 comparison of the 1984 geophysical investigations with that of 2017 suggested major, both lateral and
610 vertical, displacements of saltwater into the mainland aquifer of up to 2km and 80m respectively. The
611 thinning freshwater lens towards the sea was clearly observed. Seawater extent was larger on the
612 northern part of the study area (3 km inland from the sea) compared to the southern part. The difference
613 is inclined to variation in rainfall and geological controls. The over-pumping of coastal fresh groundwater
614 is causing a threat to the freshwater due to saltwater intrusion. Several local community hand-pumped
615 and direct buckets pulled wells exist, all of which are not metered, and abstraction can only be estimated
616 using the population around the wells. These wells are the main source of water for domestic activities
617 for the locals (rural villages) and the main contributor to water level drop and seawater intrusion along
618 the coastal coral reef strip through abstraction, which is active during the day. Over-exploitation of the
619 groundwater resource, combined with possible future decrease in rainfall and increase in temperature
620 which would affect the recharge negatively, will lead to aquifer depletion if not controlled. These, in a
621 productive aquifer such as the Kenyan South Coast will lead to water scarcity or no water for supply.
622 This will have a great effect on socio-economic development of the region. Managed aquifer recharge
623 is therefore recommended and alternative water source to ease the pressure on groundwater
624 abstraction.

625

626 *Acknowledgements*

627 We acknowledge the Royal Geographical Society (with IBG) Environment and Sustainability Research
628 Grant for financial support for all field activities. Acknowledgments extend to the Kenyan Water
629 Resources Authority (WRA) and the University of Aberdeen for supporting S. Oiro's PhD scholarship.
630 We thank Security Officers and Government of Kenya Administrators who facilitated field access by
631 informing the public of our presence in the area as well as the assistance by local casuals during the
632 geophysical surveys.

633

634

635

636

637

638

639

640

641

642

643

644

645

646

647

648 *References*

- 649 Adams, B., 1986. Tiwi Aquifer study report.pdf. Mombasa, Kenya.
- 650 Ahmed, A.H., Rayaleh, W.E., Zghibi, A., Ouddane, B., 2017. Assessment of chemical quality of
651 groundwater in coastal volcano-sedimentary aquifer of Djibouti, Horn of Africa. *J. African Earth*
652 *Sci.* 131, 284–300. doi:10.1016/j.jafrearsci.2017.04.010
- 653 Ahmed, A.T., 2017. Experimental and numerical study for seawater intrusion remediation in
654 heterogeneous coastal aquifer. *J. Environ. Manage.* 198, 221–232.
655 doi:10.1016/j.jenvman.2017.04.055
- 656 Altchenko, Y., Villholth, K.G., 2013. Transboundary aquifer mapping and management in Africa: a
657 harmonised approach. *Hydrogeol. J.* 21, 1497–1517. doi:10.1007/s10040-013-1002-3
- 658 Argamasilla, M., Barber'a, J.A., Andreo, B., 2017. Factors controlling groundwater salinization and
659 hydrogeochemical processes in coastal aquifers from southern Spain. *Sci. Total Environ.* 580,
660 50–68. doi:10.1016/j.scitotenv.2016.11.173
- 661 Arthurton, R.S., 1998. The societal value of Geoscience Information in less developed countries - The
662 Coastal Zone of Eastern Africa.pdf.
- 663 Barlow, P.M., 2003. Ground Water in Freshwater-Saltwater Environments of the Atlantic Coast. U S
664 Geol. Surv. - Circ. 1262 Circular 1, 121.
- 665 Bosch, D., Ledo, J., Bellmunt, F., Luquot, L., Gouze, P., 2016. Core-scale Electrical Resistivity
666 Tomography (ERT) monitoring of CO₂-brine mixture in Fontainebleau sandstone (under
667 revision). *J. Appl. Geophys.* 130, 23–36. doi:10.1016/j.jappgeo.2016.03.039
- 668 Buckley, D.K., 1981. Report on a visit to assess Groundwater Potential of the Kenya Coast South of
669 Malindi.
- 670 Carruthers, R.M., 1985. Report on Geophysical studies Relating to the Coastal Aquifer of the
671 Mombasa District, Kenya.
- 672 Colombani, N., Mastrocicco, M., Dinelli, E., 2015. Trace elements mobility in a saline coastal aquifer
673 of the Po river lowland (Italy). *J. Geochemical Explor.* 159, 317–328.

- 674 doi:10.1016/j.gexplo.2015.10.009
- 675 Comte, J.-C.C., Join, J.-L., Banton, O., Nicolini, E., 2014. Modelling the response of fresh
676 groundwater to climate and vegetation changes in coral islands. *J. Hydrol.* 4, 1–9.
677 doi:10.1007/s10040-014-1160-y
- 678 Comte, J.C., Cassidy, R., Obando, J., Robins, N., Ibrahim, K., Melchioly, S., Mjemah, I., Shauri, H.,
679 Bourhane, A., Mohamed, I., Noe, C., Mwega, B., Makokha, M., Join, J.L., Banton, O., Davies, J.,
680 2016. Challenges in groundwater resource management in coastal aquifers of East Africa:
681 Investigations and lessons learnt in the Comoros Islands, Kenya and Tanzania. *J. Hydrol. Reg.*
682 *Stud.* 5, 179–199. doi:10.1016/j.ejrh.2015.12.065
- 683 Hetu, R., 1978. Interpretation report: Airborne EM survey with Barringer “INPUT” system of Area 6
684 (Tiwi aquifer). Unpublished report 77-18, Terra Surveys Ltd. for Ministry of Natural Resources,
685 Mines and Geology, Kenya.
- 686 Himi, M., Tapias, J., Benabdelouahab, S., Salhi, A., Rivero, L., Elgettafi, M., El Mandour, A., Stitou, J.,
687 Casas, A., 2017. Geophysical characterization of saltwater intrusion in a coastal aquifer: The
688 case of Martil-Alila plain (North Morocco). *J. African Earth Sci.* 126, 136–147.
689 doi:10.1016/j.jafrearsci.2016.11.011
- 690 Hsieh, P.C., Hsu, H.T., Liao, C.B., Chiueh, P. Te, 2015. Groundwater response to tidal fluctuation and
691 rainfall in a coastal aquifer. *J. Hydrol.* 521, 132–140. doi:10.1016/j.jhydrol.2014.11.069
- 692 IPCC, UNEP, 1997. *The Regional Impacts of Climate Change: An Assessment of Vulnerability,*
693 *Intergovernmental Panel on Climate Change.*
- 694 Iyalomhe, F., Rizzi, J., Pasini, S., Torresan, S., Critto, A., Marcomini, A., 2015. Regional Risk
695 Assessment for climate change impacts on coastal aquifers. *Sci. Total Environ.* 537, 100–114.
696 doi:10.1016/j.scitotenv.2015.06.111
- 697 Jahanshahi, R., Zare, M., 2016. Hydrochemical investigations for delineating salt-water intrusion into
698 the coastal aquifer of Maharlou Lake, Iran. *J. African Earth Sci.* 121, 16–29.
699 doi:10.1016/j.jafrearsci.2016.05.014
- 700 Ketabchi, H., Mahmoodzadeh, D., Ataie-Ashtiani, B., Simmons, C.T., 2016. Sea-level rise impacts on

- 701 seawater intrusion in coastal aquifers: Review and integration. *J. Hydrol.* 535.
702 doi:<http://dx.doi.org/10.1016/j.jhydrol.2016.01.083>
- 703 Klassen, J., Allen, D.M., 2017. Assessing the risk of saltwater intrusion in coastal aquifers. *J. Hydrol.*
704 doi:[10.1016/j.jhydrol.2017.02.044](https://doi.org/10.1016/j.jhydrol.2017.02.044)
- 705 Kuria, Z., 2013. Groundwater Distribution and Aquifer Characteristics in Kenya. *Kenya A Nat. Outlook*
706 - *Geo-Environmental Resour. Hazards* 16, 83–107. doi:[10.1016/B978-0-444-59559-1.00008-6](https://doi.org/10.1016/B978-0-444-59559-1.00008-6)
- 707 Lathashri, U.A., Mahesha, A., 2015. Simulation of Saltwater Intrusion in a Coastal Aquifer in
708 Karnataka, India. *Aquat. Procedia* 4, 700–705. doi:[10.1016/j.aqpro.2015.02.090](https://doi.org/10.1016/j.aqpro.2015.02.090)
- 709 Martínez-Moreno, F.J., Monteiro-Santos, F.A., Bernardo, I., Farzadian, M., Nascimento, C.,
710 Fernandes, J., Casal, B., Ribeiro, J.A., 2017. Identifying seawater intrusion in coastal areas by
711 means of 1D and quasi–2D joint inversion of TDEM and VES data. *J. Hydrol.* 552, 609–619.
712 doi:[10.1016/j.jhydrol.2017.07.026](https://doi.org/10.1016/j.jhydrol.2017.07.026)
- 713 Melloul, A.J., Goldenberg, L.C., 1997. Monitoring of seawater intrusion in coastal aquifers: Basics and
714 local concerns. *J. Environ. Manage.* 51, 73–86. doi:[10.1006/jema.1997.0136](https://doi.org/10.1006/jema.1997.0136)
- 715 Mumma, A., Lane, M., Kairu, E., Tuinhof, A., Hirji, R., 2011. Kenya, Groundwater Governance case
716 study.
- 717 Mwakamba, C., Njuguna, A., Oiro, S., Ndung'u, A., Ang'weya, R., Hamisi, W., Mutinda, J., Mwangi,
718 S., 2014. *Tiwi Aquifer Water Resources Assessment Report*. Nairobi, Kenya.
- 719 Oiro, S., Comte, J.-C., Soulsby, C., Walraevens, K., 2018. Using stable water isotopes to identify
720 spatio-temporal controls on groundwater recharge in two contrasting East African aquifer
721 systems. *Hydrol. Sci. J.* 63, 1–16. doi:[10.1080/02626667.2018.1459625](https://doi.org/10.1080/02626667.2018.1459625)
- 722 Post, V.E.A., Werner, A.D., 2017. Coastal Aquifers: Scientific Advances in the face of Global
723 Environmental Challenges. *J. Hydrol.* 551, 1–3. doi:[10.1016/j.jhydrol.2017.04.046](https://doi.org/10.1016/j.jhydrol.2017.04.046)
- 724 Priyanka, B.N., Mahesha, A., 2015. Parametric Studies on Saltwater Intrusion into Coastal Aquifers
725 for Anticipate Sea Level Rise. *Aquat. Procedia* 4, 103–108. doi:[10.1016/j.aqpro.2015.02.015](https://doi.org/10.1016/j.aqpro.2015.02.015)
- 726 Sauret, E.S.G., Beaujean, J., Nguyen, F., Wildemeersch, S., Brouyere, S., 2015. Characterization of
727 superficial deposits using electrical resistivity tomography (ERT) and horizontal-to-vertical

- 728 spectral ratio (HVSZ) geophysical methods: A case study. *J. Appl. Geophys.* 121, 140–148.
729 doi:<http://dx.doi.org/10.1016/j.jappgeo.2015.07.012>
- 730 Sincat-Atkins, 1996. Second Mombasa & Coastal Water Supply Engineering and rehabilitation
731 project. Bulk water (source works) supply Development.
- 732 Sonkamble, S., Chandra, S., Ahmed, S., Rangarajan, R., 2014. Source speciation resolving
733 hydrochemical complexity of coastal aquifers. *Mar. Pollut. Bull.* 78, 118–129.
734 doi:[10.1016/j.marpolbul.2013.10.052](https://doi.org/10.1016/j.marpolbul.2013.10.052)
- 735 Steyl, G., Dennis, I., 2010. Review of coastal-area aquifers in Africa. *Hydrogeol. J.* 18, 217–225.
736 doi:[10.1007/s10040-009-0545-9](https://doi.org/10.1007/s10040-009-0545-9)
- 737 Tahal, G., Bhundia, A., 2012. R EPUBLIC OF K ENYA Water and Sanitation Service Improvement
738 Project (WaSSIP) Consultancy Services for Water Supply Master Plan for Mombasa and Other
739 Towns Within Coast Province. Mombasa, Kenya.
- 740 Taylor, C.J., Alley, W.M., 2001. Ground-water-level monitoring and the importance of long-term water-
741 level data. *Geol. Surv. Circ.* 1–76.
- 742 Taylor, R.G., Scanlon, B., Doll, P., Rodell, M., van Beek, R., Wada, Y., Longuevergne, L., Leblanc,
743 M., Famiglietti, J.S., Edmunds, M., Konikow, L., Green, T.R., Chen, J.Y., Taniguchi, M.,
744 Bierkens, M.F.P., MacDonald, A., Fan, Y., Maxwell, R.M., Yechieli, Y., Gurdak, J.J., Allen, D.M.,
745 Shamsudduha, M., Hiscock, K., Yeh, P.J.F., Holman, I., Treidel, H., 2012. Ground water and
746 climate change, in: *Nature Climate Change*. pp. 322–329. doi:[10.1038/nclimate1744](https://doi.org/10.1038/nclimate1744)
- 747 Tole, M.P., 1997. Pollution of groundwater in the coastal Kwale District, Kenya, Sustainability of Water
748 Resources under Increasing Uncertainty (Proceedings of the Rabat Symposium S1, April 1997).
749 IAHS Publ. no. 240, 1997.
- 750 Wangati, F.J., Said, M.Y., 1997. National Land Degradation Assessment and Mapping in Kenya.
751

Coastal aquifers in East Africa are under pressure from increasing water demand driven by unprecedented demographic growth

Extent and drivers of saltwater intrusion were investigated in a strategic aquifer of South Coast Kenya

Long-term records showed that groundwater abstraction is the primary driver of boreholes salinization over time

Groundwater mapping demonstrated that geology and groundwater abstraction dictate regional patterns of salinity

Geophysical investigations provided estimates of the extent and rate of the inland advancement of the saltwater front over the last 30 years